Copyright © 1973 American Telephone and Telegraph Company
The Bell System Technical Journal
Vol. 52, No. 6, July–August, 1973
Printed in U.S.A.

Receiver Design for Digital Fiber Optic Communication Systems, I

By S. D. PERSONICK

(Manuscript received January 15, 1973)

This paper is concerned with a systematic approach to the design of the "linear channel" of a repeater for a digital fiber optic communication system. In particular, it is concerned with how one properly chooses the front-end preamplifier and biasing circuitry for the photodetector; and how the required power to achieve a desired error rate varies with the bit rate, the received optical pulse shape, and the desired baseband-equalized output pulse shape.

It is shown that a proper front-end design incorporates a high-impedance preamplifier which tends to integrate the detector output. This must be followed by proper equalization in the later stages of the linear channel. The baseband signal-to-noise ratio is calculated as a function of the preamplifier parameters. Such a design provides significant reduction in the required optical power and/or required avalanche gain when compared to a design which does not integrate initially.

It is shown that, when the received optical pulses overlap and when the optical channel is behaving linearly in power,[1] baseband equalization can be used to separate the pulses with a practical but significant increase in required optical power. This required power penalty is calculated as a function of the input and equalized pulse shapes.

I. INTRODUCTION

The purpose of this paper is to provide insight into a systematic approach to designing the "linear channel" of a repeater for a digital fiber optic communication system.

In particular, we are interested in how one properly chooses the biasing circuitry for the photodetector; and how the required power to achieve a desired error rate varies with the bit rate, the received optical pulse shape, and desired baseband output pulse shape.

Throughout this paper, performance will be measured in terms of signal-to-noise ratios. Efforts to calculate exact error rates and bounds

to error rates are difficult to carry out, and, in the past, the results of such efforts have shown little deviation (for practical design purposes) from calculations of error rates using the signal-to-noise ratio (Gaussian approximation) approach. (See Refs. 2 through 5 and Appendix A.)

II. INPUT–OUTPUT RELATIONSHIPS FOR AN AVALANCHE DETECTOR

An avalanche photodiode is the device of interest in fiber applications for converting optical power into current for amplification and equalization, ultimately to produce a baseband voltage for regeneration.

In order to appreciate its performance in practical optical systems, we have to characterize the avalanche photodiode from three points of view: the physical viewpoint, the circuit viewpoint, and the statistical viewpoint.

When we study the device from the physical viewpoint, we ask how does it operate, how do we develop circuit and statistical models of its operation, and what are the limitations of the models.

From the circuit viewpoint, we investigate how to design a piece of equipment in which the device will perform some function.

From the statistical viewpoint, we investigate the probabilistic behavior of the device to allow us to quantify its performance in a circuit.

2.1 *The Physical Viewpoint*

The avalanche photodiode is a semiconductor device which is normally operated in a backbiased manner–producing a region within the device where there is a high field (see Fig. 1). Due to thermal agitation and/or the presence of incident optical power, pairs of holes and electrons can be generated at various points within the diode. These carriers drift toward opposite ends of the device under the influence of the applied field. When a carrier passes through the high-field region, it may gain sufficient energy to generate one or more new pairs of holes and electrons through collision ionization. These new pairs can in turn generate additional pairs by the same mechanism. Carriers accumulate at opposite ends of the diode, thereby reducing the potential across the device until they are removed by the biasing and other circuitry in parallel with the diode (see Fig. 2). The chances that a carrier will generate a new pair when passing through the high-field region depends upon the type of carrier (hole or electron), the material out of which the diode is constructed, and the voltage across the device. To the extent that carriers do not accumulate to significantly modulate the

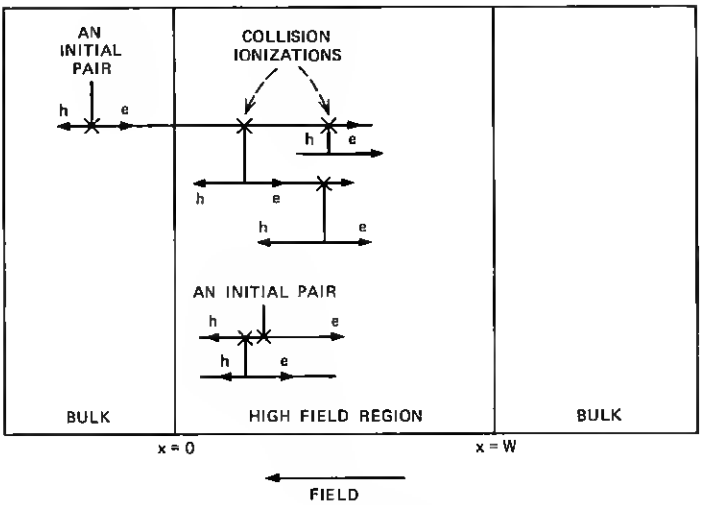

Fig. 1—Avalanche detector.

voltage across the device, it can be assumed that all ionizing collisions are statistically independent. This assumption also requires that the mean time between ionizing collisions be large compared to the time it takes for a carrier in the high-field region to randomize its momentum.

2.2 *The Circuit Viewpoint*

From the discussion above, and of course more detailed investigations,[3,6–8] it has been concluded that a reasonable small-signal model of an avalanche photodiode with a biasing circuit shown in Fig. 2 is the equivalent circuit of Fig. 3. In Fig. 3, C_d is the junction capacitance of the diode† across which voltage accumulates when charges produced within the device separate under the influence of the bias field. The current generator $i(t)$ represents the production of charges (holes and electrons) by optical and thermal generation and collision ionization in the diode high-field region. In order to use the photodiode efficiently,

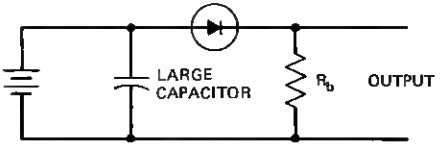

Fig. 2—Detector biasing circuit.

† Not to be confused with the large power supply bypass capacitor of Fig. 2.

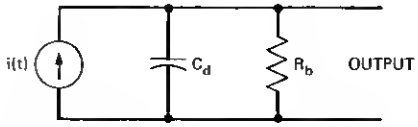

Fig. 3—Equivalent circuit of biased detector.

we must design a circuit which will respond to the current $i(t)$ with as little distortion and added noise as possible.

In order to derive information from the circuit responding to $i(t)$, we must understand the statistical relationship between $i(t)$ (the equivalent current generator) and the incident optical power $p(t)$.

2.3 *The Statistical Viewpoint*

In Fig. 3, the current source $i(t)$ can be considered to be a sequence of impulses corresponding to electrons generated within the photodiode due to optical or thermal excitation or collision ionization. We shall now specify, in a statistical way, how many electrons are produced and when they are produced.

From various physical studies,[3,7,9] it has been concluded that for cases of current interest the electron production process can be modeled as shown in Fig. 4.

Let the optical power falling upon the photon counter be $p(t)$.† In response to this power and due to thermal effects, the photon counter of Fig. 4 produces electrons at average rate $\lambda(t)$ per second where

$$\lambda(t) = [(\eta/\hbar\Omega)p(t)] + \lambda_0, \tag{1}$$

where

η = photon counter quantum efficiency
$\hbar\Omega$ = energy of a photon
λ_0 = dark current "counts" per second.

$\lambda(t)$ is only the average rate at which electrons are produced. In any interval T seconds long, the probability that exactly N counts are produced is given by

$$P[N, (t_0, t_0 + T)] = \frac{\Lambda^N e^{-\Lambda}}{N!},$$

where

$$\Lambda = \int_{t_0}^{t_0+T} \lambda(t)dt. \tag{2}$$

† The reader is cautioned not to confuse $p(t)$, the optical power, with the probability densities (e.g., $P[N, \{t_k\}]$) in this paper.

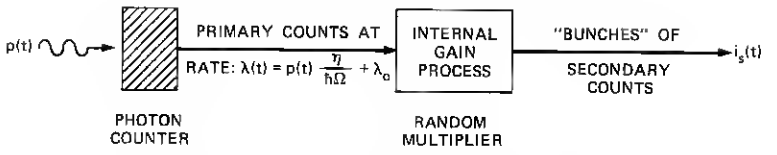

Fig. 4—Model of $i_s(t)$ generation process.

Given $p(t)$, the numher of electrons produced in any interval is statistically independent of the numher produced in any other disjoint interval.

A process of impulse (electron) production satisfying (2) and the ahove independent increments condition is said to he a "Poisson impulse process" with arrival rate $\lambda(t)$.[10]

A useful equivalent description of the ahove process follows.

If T is an interval, the probahility that exactly N electrons will he produced at the (approximate) times $t_1 \pm \frac{1}{2}\Delta$, $t_2 \pm \frac{1}{2}\Delta$, $\cdots$ $t_N \pm \frac{1}{2}\Delta$ where the widths Δ are very small is

$$P[N, \{t_k\}] = \{e^{-\Lambda} \prod_1^N [\lambda(t_k)\Delta]/N!\} + o(\Delta), \tag{3}$$

where Λ is defined in (2) and $o(\Delta)$ is a term such that

$$\lim_{\Delta \to 0} \frac{o(\Delta)}{\Delta} = 0.$$

It is *important* to note that in (3) the times $\{t_k\}$ are *not* in order, that is, in (3) it is *not* necessarily true that $t_1 < t_2$, etc.

Each of the "primary" impulses (electrons) produced hy the photon counter enters a random multiplier where, corresponding to collision ionization, it is replaced hy g contiguous "secondary" impulses (electrons). The numher g is governed hy the statistics of the internal gain mechanism of the photodiode. Each primary impulse (electron) is "multiplied" in this manner by a value g which is statistically independent of the value g assigned to other primaries.

Thus the current leaving the photodiode consists of "hunches" of electrons, the numher of electrons in the hunch heing a random quantity having statistics to he descrihed helow. For applications of interest here, it will he assumed that all electrons in a hunch exit the photodiode at the time when the primary is produced. This implies that the duration of the photodiode response to a single primary hole-electron pair is very short compared to the response times of circuitry to he used with the photodiode.

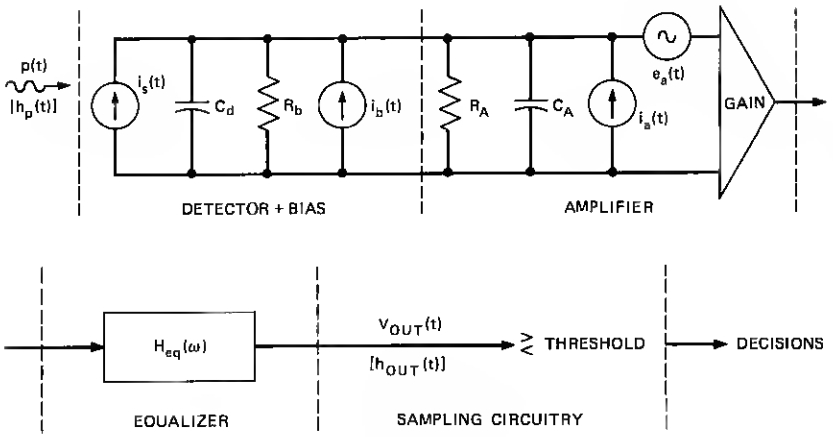

Fig. 5—Receiver.

Different avalanche photodiodes have different statistics governing the number of electrons in a bunch, i.e., the gain. For applications below, we will only need to know the mean gain $\langle g \rangle$ and the mean square gain $\langle g^2 \rangle$. For a large class of avalanche photodiodes of interest, it has been found that[3,7]

$$\langle g^2 \rangle \cong \langle g \rangle^{2+x}, \tag{4}$$

where $\langle g \rangle$ is determined by the applied bias voltage and x, a number usually between 0 and 1, depends upon the materials out of which the diode is constructed. For germanium photodiodes, $x \cong 1$; for well-designed silicon photodiodes, $x \approx 0.5$.

III. AN OPTICAL RECEIVER

Figure 5 shows a fairly typical receiver, in schematic form, consisting of an avalanche photodiode, an amplifier, and an equalizer.

The amplifier is modeled as an ideal high-gain infinite-impedance amplifier with an equivalent shunt capacitance and resistance at the input and with two noise sources referred to the input. For the purposes of this paper, the noise sources will be assumed to be white, Gaussian, and uncorrelated. Extensions to other amplifier models will be straightforward when the techniques of this paper are understood.†

It is assumed that the amplifier gain is sufficiently high so that noises introduced by the equalizer are negligible.

† With this model, the noise sources of the amplifier do not change when the input and output load circuitry changes.

The power falling upon the detector will he assumed to be of the form of a digital pulse stream

$$p(t) = \sum_{-\infty}^{\infty} b_k h_p(t - kT), \tag{5}$$

where b_k takes on one of two values for each integer value of k, T = the pulse spacing, $h_p(t - kT)$ = pulse shape and is positive for all t. We shall assume $\int_{-\infty}^{\infty} h_p(t - kT)dt = 1$, therefore b_k is the energy in pulse k. The assumption that the received power will be in the form (5) appears reasonahle for intensity modulation and fiher systems of interest.[1]

From (1) we have the average detector output current $\langle i_s(t)\rangle$ given by

$$\langle i_s(t)\rangle = \frac{\eta\langle g\rangle ep(t)}{\hbar\Omega} + \langle g\rangle e\lambda_0,$$

where

$\langle g\rangle$ = average detector internal gain

e = electron charge

λ_0 = dark current electrons per second

$\frac{\eta}{\hbar\Omega} p(t)$ = average optical primary electrons per second.

Therefore, the average voltage (neglecting dc components) at the equalizer output is

$$\langle v_{\text{out}}(t)\rangle = \frac{A\eta\langle g\rangle ep(t)}{\hbar\Omega} * h_{\text{fe}}(t) * h_{\text{eq}}(t), \tag{6}$$

where "$*$" indicates convolution and A is an arbitrary constant.

$$h_{\text{fe}}(t) = F\left\{\frac{1}{\frac{1}{R_T} + j\omega(C_d + C_A)}\right\}$$

= amplifier input circuit current impulse response,

$$R_T = \left[\frac{1}{R_b} + \frac{1}{R_A}\right]^{-1} = \text{total detector parallel load resistance,}$$

and $h_{\text{eq}}(t)$ = equalizer impulse response.

Clearly, $\langle v_{\text{out}}(t)\rangle$ is of the form

$$\langle v_{\text{out}}(t)\rangle = \sum_{-\infty}^{\infty} b_k h_{\text{out}}(t - kT) \tag{7}$$

and $v_{out}(t)$ is of the form

$$v_{out}(t) = \sum_{-\infty}^{\infty} b_k h_{out}(t - kT) + n(t),$$

where $n(t)$ represents *deviations* (or noises) of $v_{out}(t)$ from its average.

The fundamental task ahead is to pick R_b (the bias circuit resistor) and $h_{eq}(t)$ so that a system which samples $v_{out}(t)$ at the times $\{kT\}$ can make decisions as to which value b_k has assumed (by comparing the sample to a threshold) with minimum chance of error.

IV. CALCULATING SIGNAL–TO–NOISE RATIO IN TERMS OF THE EQUALIZED PULSE SHAPE

Having defined the receiver and its statistics in the above sections, we can now calculate the variance of $n(t)$, the noise portion of the output $v_{out}(t)$ of the system of Fig. 5, defined as follows:

$$N = \langle (n(t))^2 \rangle = \langle v_{out}^2(t) \rangle - \langle v_{out}(t) \rangle^2. \tag{8}$$

The noise, N, of (8) above depends upon the coefficients $\{b_k\}$ defined in (5) and upon the time t.

We shall first of all restrict consideration to the set of times $t = \{kT\}$ when a decision as to the values $\{b_k\}$ will be made hy sampling $v_{out}(t)$. We shall next assume that the equalized pulses satisfy

$$\begin{aligned} h_{out}(0) &= 1 \\ h_{out}(t) &= 0 \qquad \text{for} \qquad t = kT, \qquad k \neq 0. \end{aligned} \tag{9}$$

That is, we shall assume that the equalized pulse stream has no intersymbol interference at the sampling times kT.† Therefore,

$$v_{out}(kT) = b_k + n(kT). \tag{10}$$

In eq. (10) the noise, $n(t)$, still depends upon all the $\{b_k\}$ and the time t. This is a property which distinguishes fiber optic systems from many other systems where the noise is signal-independent and stationary (not time-dependent). Consider, without loss of generality, the output, $v(t)$, at $t = 0$. We define the worst-case noise, $NW(b_0)$, for each of the two possible values of b_0 as follows:

$$NW(b_0) = \max_{\{b_k\}, k \neq 0} [\langle v_{out}^2(0) \rangle - \langle v_{out}(0) \rangle^2], \tag{11}$$

where in (11) the maximization is over all possible sets $\{b_k\}$ for $k \neq 0$, and where b_0 can take on either of two values as previously stated. The

† The limitations imposed by this assumption are discussed in Section VII.

quantity $NW(b_0)$ shows, for the two possihle values of b_0, what the noise for the worst comhination of the other symhols is.

We shall next calculate $\langle v_{\text{out}}^2(t)\rangle - \langle v_{\text{out}}(t)\rangle^2$ as a function of the set $\{b_k\}$.

Examine Fig. 5. We shall define the two-sided spectral density of the amplifier-current noise source $i_a(t)$ as S_I and the two-sided spectral height of the amplifier-voltage noise source $e_a(t)$ as S_E. The two-sided spectral density of the Johnson-current noise source $i_b(t)$ associated with R_b is $2k\theta/R_b$, where k is Boltzmann's constant and θ is the ahsolute temperature.

We can write the output noise as follows:

$$v_{\text{out}}(t) - \langle v_{\text{out}}(t)\rangle = n_S(t) + n_R(t) + n_I(t) + n_E(t), \tag{12}$$

where

$n_S(t)$ is the output noise due to the random multiplied Poisson process nature of the current $i_s(t)$ produced hy the detector,

$n_R(t)$ is the output noise due to the Johnson noise current source of the resistor R_b,

$n_I(t)$ is the output noise due to the amplifier input current noise source $i_a(t)$, and

$n_E(t)$ is the output noise due to the amplifier input voltage noise source $e_a(t)$.

We have

$$\begin{aligned}
&\langle v_{\text{out}}^2(t)\rangle - \langle v_{\text{out}}(t)\rangle^2 \\
&\quad = \langle (v_{\text{out}}(t) - \langle v_{\text{out}}(t)\rangle)^2\rangle \\
&\quad = \langle n_S^2(t)\rangle + \langle n_R^2(t)\rangle + \langle n_I^2(t)\rangle + \langle n_E^2(t)\rangle \\
&\quad = \langle n_S^2(t)\rangle + (2k\theta/R_b)\frac{1}{2\pi}\int_{-\infty}^{\infty}\left|H_{\text{eq}}(\omega)\,\frac{1}{\frac{1}{R_b}+\frac{1}{R_A}+j\omega(C_d+C_A)}\right|^2 d\omega \\
&\qquad + (S_I)\frac{1}{2\pi}\int_{-\infty}^{\infty}\left|H_{\text{eq}}(\omega)\,\frac{1}{\frac{1}{R_b}+\frac{1}{R_A}+j\omega(C_d+C_A)}\right|^2 d\omega \\
&\qquad + (S_E)\frac{1}{2\pi}\int_{-\infty}^{\infty}|H_{\text{eq}}(\omega)|^2 d\omega.
\end{aligned} \tag{13}$$

In (13), the last three terms were evaluated using the well-known formula for the average-squared output of a filter driven hy white noise. We must now calculate the "shot noise" term $\langle n_S^2(t)\rangle$.

Recall that $i_s(t)$ consists of impulses of random charge corresponding to "bunches" of electrons with a random numher g per bunch, this numher heing independent from hunch to hunch.

Consider a finite interval of duration L. Let g_k be the number of electrons in bunch k in the interval; where the bunches are labeled *not* in order of time but at random. Let t_k be the arrival time of bunch k. Let $h_I(t)$ be the response of the RC circuit, amplifier, equalizer combination to a current impulse from $i_s(t)$. Then the output $v_{out}(t)$ *just due to the current* $i_s(t)$ *in the interval* L is

$$v_{out}^{L}(t) = \sum_{1}^{N} e g_k h_I(t - t_k), \tag{14}$$

where N is the number of bunches.

Recall that the probability density of N bunches at the times $\{t_k\}$ is

$$p[N, \{t_k\}] = \frac{e^{-\Lambda} \prod_{1}^{N} \lambda(t_k)}{N!}, \tag{15}$$

where

$$\lambda(t) = p(t) \frac{\eta}{\hbar\Omega} + \lambda_0.$$

Thus combining (14) and (15) and leaving out some tedious algebra we obtain[10]

$$\langle v_{out}^{L}(t) \rangle = \int_{\text{interval } L} e\langle g \rangle (p(t')\eta/\hbar\Omega + \lambda_0) h_I(t - t')dt'. \tag{16}$$

In a similar manner, we obtain

$$\langle (v_{out}^{L}(t))^2 \rangle - \langle v_{out}^{L}(t) \rangle^2 = \int_{\text{interval } L} e^2\langle g^2 \rangle \left(p(t') \frac{\eta}{\hbar\Omega} + \lambda_0 \right) h_I^2(t - t')dt,$$

where $\langle g \rangle$ is the mean internal gain of the detector and $\langle g^2 \rangle$ is the mean-squared internal gain.

We therefore obtain, letting $L \to \infty$, the result

$$\langle n_S^2(t) \rangle = \lim_{L \to \infty} [\langle [v_{out}^{L}(t)]^2 \rangle - \langle v_{out}^{L}(t) \rangle^2]$$

$$= \int_{-\infty}^{\infty} e^2\langle g^2 \rangle \left\{ [\sum b_k h_p(t' - kT)] \frac{\eta}{\hbar\Omega} + \lambda_0 \right\} h_I^2(t - t')dt'. \tag{17}$$

Further,

$$H_I(\omega) = F\{h_I(t - t')\} = H_{eq}(\omega) \frac{1}{\frac{1}{R_b} + \frac{1}{R_A} + j\omega(C_d + C_A)}. \tag{18}$$

Thus we have the remaining term in (13) in terms of the input optical pulse, the equalizer response, and the RC circuit at the amplifier input.

Converting everything to the frequency domain and recalling that we have normalized the equalized output pulse $h_{out}(t)$ to unity at $t = 0$, we obtain

$$NW(b_0) = \max_{\{b_k, k \neq 0\}} \left[\left(\frac{1}{2\pi} \right)^2 \int_{-\infty}^{\infty} \frac{\langle g^2 \rangle}{\langle g \rangle^2} \frac{\hbar\Omega}{\eta} H_p(\omega) \left(\sum_{-\infty}^{\infty} b_k e^{j\omega kT} \right) \right.$$

$$\times \left(\frac{H_{out}(\omega)}{H_p(\omega)} * \frac{H_{out}(\omega)}{H_p(\omega)} \right) d\omega$$

$$+ \frac{(\hbar\Omega/\eta)^2}{2\pi \langle g \rangle^2 e^2} \left(\frac{2k\theta}{R_b} + S_I + e^2 \langle g^2 \rangle \lambda_0 \right) \int_{-\infty}^{\infty} \left| \frac{H_{out}(\omega)}{H_p(\omega)} \right|^2 d\omega$$

$$\left. + \frac{(\hbar\Omega/\eta)^2}{2\pi \langle g \rangle^2 e^2} S_E \int_{-\infty}^{\infty} \left| \frac{H_{out}(\omega) \left(\frac{1}{R_b} + \frac{1}{R_A} + j\omega(C_d + C_A) \right)}{H_p(\omega)} \right|^2 d\omega \right], \quad (19)$$

where

$H_p(\omega) = F\{h_p(t)\}$ = input power pulse transform,
$H_{out}(\omega) = F\{h_{out}(t)\}$ = output pulse transform,
"$*$" = convolution,
b_0 = coefficient multiplying zeroth input pulse,

and

$$\frac{1}{2\pi} \int_{-\infty}^{\infty} H_{out}(\omega) d\omega = 1. \quad (20)$$

In principle, we wish to minimize $NW(b_0)$ by choosing R_b and $H_{eq}(\omega)$ for the worst-case combination of symbols $\{b_k\}$, subject to the zero intersymbol interference condition on the ouput pulse stream $v_{out}(t)$ [recognizing that we have normalized $h_{out}(t)$ and $H_{out}(\omega)$ as given in (9) and (20) above].

4.1 *Comments*

(*i*) One observation, which follows regardless of the choice of $H_{out}(\omega)$, is that the noise is always made smaller when R_b is increased. Therefore, subject to practical constraints and for a fixed amplifier and a fixed desired output pulse shape (which is determined by the equalizer and R_b), it is always best to make R_b, the bias circuit resistor, as large as possible.

(*ii*) It is also clear, from (17) and the fact that the input pulse $h_p(t)$ is positive for all t, that the worst-case noise occurs when all the b_k (except b_0) assume the larger of the two possible

values. Recall that we are interested in the noise for hoth values of b_0.

(*iii*) Furthermore, for a given S_E and S_I and a given output pulse shape, it is desirahle that the amplifier input resistance he as large as possihle and that the amplifier shunt capacitance he as small as possihle.

(*iv*) It is desirahle that the diode shunt capacitance be as small as possihle.

V. CHOOSING THE EQUALIZED PULSE SHAPE

In principle, using (19) and given $H_p(\omega)$, $\langle g \rangle$, $\langle g^2 \rangle$, S_I, S_E, R_b, R_A, C_d, and C_A one can find the equalized pulse shape $H_{\text{out}}(\omega)$ for each value of b_0 that minimizes the worst-case noise.

In practice, other considerations in addition to the noise are also of interest. In particular, it is important not only that the intersymhol interference he low at the nominal decision times kT, but that it he sufficiently small at times offset from $\{kT\}$ to allow for timing errors in the sampling process.

Therefore, rather than seeking the equalized pulse shape that minimizes the noise, we shall consider various equalized pulse shapes to see how the noise trades off against eye width.

Before proceeding, it is helpful to perform some normalizations upon (19) to reduce the number of parameters.

Make the following definitions:

$$R_T = \left(\frac{1}{R_b} + \frac{1}{R_A}\right)^{-1} = \text{total detector parallel load resistance,} \tag{21}$$

$C_T = C_d + C_A =$ total detector parallel load capacitance,
$b_{\max} =$ larger value of b_k, $b_{\min} =$ smaller value of b_k,

$$H_p'(\omega) = H_p\left(\frac{2\pi\omega}{T}\right),$$

$$H_{\text{out}}'(\omega) = \frac{1}{T} H_{\text{out}}\left(\frac{2\pi\omega}{T}\right).$$

In this normalization, the functions $H_p'(\omega)$ and $H_{\text{out}}'(\omega)$ depend only upon the *shapes* of $H_p(\omega)$ and $H_{\text{out}}(\omega)$, not upon the time slot width T. The previous normalizing conditions on $H_p(\omega)$ and $H_{\text{out}}(\omega)$ imply conditions on $H_p'(\omega)$ and $H_{\text{out}}'(\omega)$

$$H_p(0) = 1 \Rightarrow H_p'(0) = 1 \tag{22}$$

which implies

$$\int_{-\infty}^{\infty} h_p(t)dt = 1.$$

Also,

$$h_{\text{out}}(0) = 1 \Rightarrow \frac{1}{2\pi}\int_{-\infty}^{\infty} H_{\text{out}}(\omega)d\omega = 1 \Rightarrow \int_{-\infty}^{\infty} H'_{\text{out}}(f)df = 1.$$

With the above normalizations, (19) becomes

$$NW(b_0) = \left(\frac{\hbar\Omega}{\eta}\right)^2 \left\{ \frac{\langle g^2\rangle}{\langle g\rangle^2}\frac{\eta}{\hbar\Omega}\,[\overset{\text{SHOT NOISES}}{\overbrace{b_0 I_1 + b_{\max}[\Sigma_1 - I_1]}}] \right.$$

$$+ \frac{T}{(\langle g\rangle e)^2}\left[S_I + \frac{2k\theta}{R_b} + \overset{\text{SHOT NOISE}}{\overbrace{\langle g^2\rangle e^2\lambda_d}} + \frac{S_E}{R_T^2}\right] I_2$$

$$\left. + \frac{(2\pi C_T)^2 S_E I_3}{T(\langle g\rangle e)^2}\right\}, \qquad \overset{\text{THERMAL NOISES}}{\overbrace{}} \tag{23}$$

where

$$I_1 = \int_{-\infty}^{\infty} H'_p(f)\left[\frac{H'_{\text{out}}(f)}{H'_p(f)} * \frac{H'_{\text{out}}(f)}{H'_p(f)}\right] df$$

$$\Sigma_1 = \sum_{k=-\infty}^{\infty} H'_p(k)\left[\frac{H'_{\text{out}}(k)}{H'_p(k)} * \frac{H'_{\text{out}}(k)}{H'_p(k)}\right]$$

$$I_2 = \int_{-\infty}^{\infty}\left|\frac{H'_{\text{out}}(f)}{H'_p(f)}\right|^2 df$$

$$I_3 = \int_{-\infty}^{\infty}\left|\frac{H'_{\text{out}}(f)}{H'_p(f)}\right|^2 f^2 df.$$

In (23), the first shot-noise term is due to the pulse in the time slot under decision, the second term being shot noises from the other pulses which are assumed to be all "on." From this normalized form of (19), we see that for a fixed input pulse *shape* and a fixed output pulse *shape* and with fixed R_b, R_A, C_T, S_E, and S_I, the noise decreases as the bit rate, $1/T$, increases (a consequence of the square-law detection) until the term involving I_3 dominates. After that, the noise increases with increasing bit rate (due to the shunt capacitance C_T).

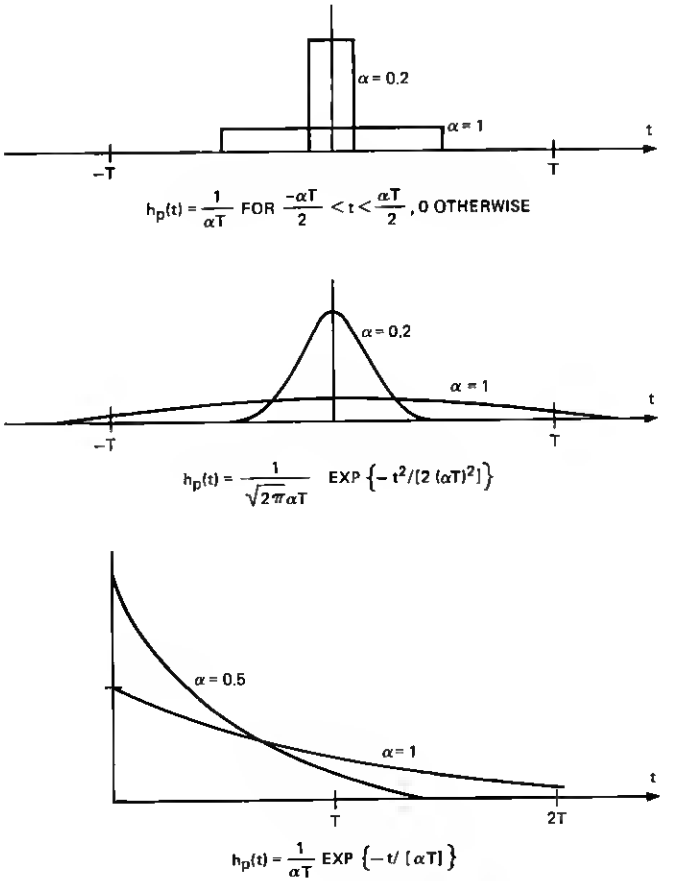

Fig. 6a—Input pulse families.

Example of Normalization:

Suppose the input optical pulse is a rectangular pulse of unit area having width equal to one-half a time slot T; then

$$\begin{aligned} H_p(\omega) &= \int_{-\frac{1}{4}T}^{\frac{1}{4}T} \frac{2}{T} e^{i\omega t} dt \\ &= \frac{1}{i\omega}\left(\frac{2}{T}\right)(e^{i\omega T/4} - e^{-i\omega T/4}) \\ &= \sin\frac{(\omega T/4)}{\omega T/4}. \end{aligned} \tag{24}$$

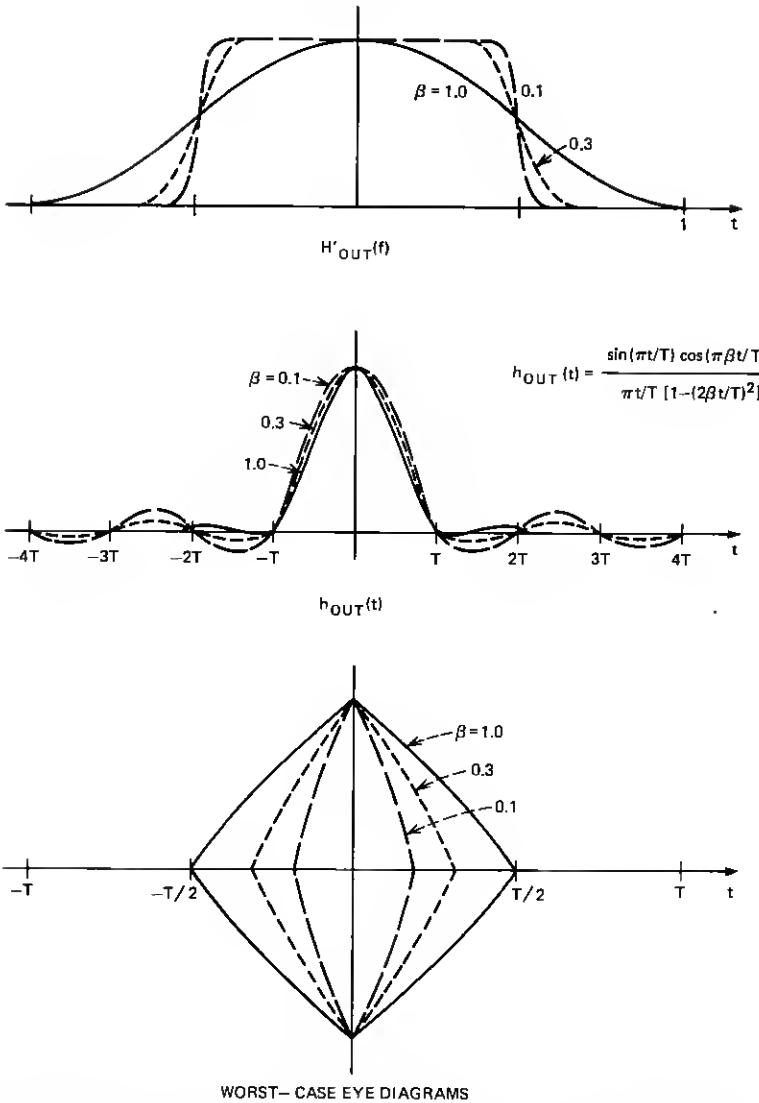

Fig. 6b—Frequency domain, time domain, and eye diagram representations of raised cosine family.

Therefore,

$$H_p'(f) = H_p\left(\frac{2\pi f}{T}\right) = \frac{\sin(\pi f/2)}{\pi f/2}.$$

As expected, the normalized pulse spectrum $H_p'(f)$ is independent of the time slot width T and merely reflects the fact that the pulse $h_p(t)$ is a rectangular pulse with width equal to half a time slot.

In order to obtain the noise for various input and output (equalized) pulse shapes, one needs to calculate the three integrals I_1, I_2, and I_3 and the sum $\sum_1$.

Consider the following three families of input pulse shapes (see Fig. 6a) and single family of output pulse shapes (see Fig. 6b).

(*i*) Rectangular input pulses:

$$h_p(t) = \frac{1}{\alpha T}, \qquad -\frac{\alpha T}{2} < t < \frac{\alpha T}{2}, \qquad 0 \text{ otherwise} \tag{25}$$

$$H_p'(f) = \frac{\sin(\alpha\pi f)}{\alpha\pi f}.$$

(*ii*) Gaussian input pulses:

$$h_p(t) = \frac{1}{\sqrt{2\pi}\alpha T} e^{-[t^2/2(\alpha T)^2]}$$

$$H_p'(f) = e^{-(2\pi\alpha f)^2/2}.$$

(*iii*) Exponential input pulses:

$$h_p(t) = \frac{1}{\alpha T} e^{-t/\alpha T}$$

$$H_p'(f) = \frac{1}{1 + j2\pi\alpha f}.$$

(*iv*) "Raised cosine" output pulses:

$$h_{\text{out}}(t) = \left[\sin\left(\frac{\pi t}{T}\right)\cos\left(\frac{\pi\beta t}{T}\right)\right]\left[\frac{\pi t}{T}\left(1 - \left(\frac{2\beta t}{T}\right)^2\right)\right]^{-1}$$

$$H_{\text{out}}'(f) = 1, \qquad \text{for} \qquad 0 < |f| < \frac{(1-\beta)}{2}$$

$$= \frac{1}{2}\left[1 - \sin\left(\frac{\pi f}{\beta} - \frac{\pi}{2\beta}\right)\right], \qquad \text{for } \frac{1-\beta}{2} < |f| < \frac{1+\beta}{2}$$

$$= 0 \text{ otherwise.}$$

(Time, frequency, and eye diagram representations of the raised cosine family are shown as a function of β in Fig. 6b.[11])

In Figs. 7 through 18 calculations of I_1, I_2, I_3, and I_4 are given graphically for each input pulse family as a function of α and β.

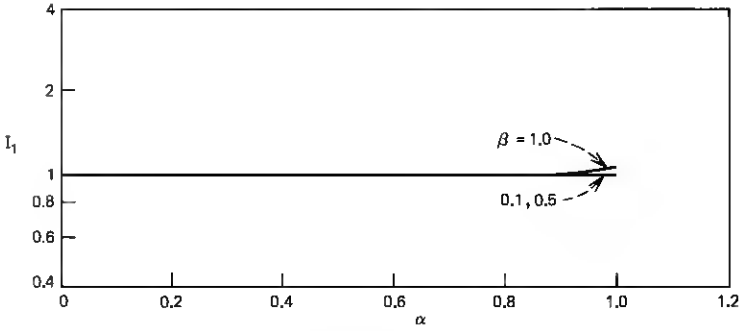

Fig. 7—Rectangular family I_1 vs α and β.

5.1 *Comments on the Numerical Results*

For the rectangular input pulses with widths between 0.1 and 1 time slot, I_1, $\sum_1$, I_2, and I_3 vary very little. Thus, if one expects to receive rectangular optical pulses which are fixed in energy, the required energy per pulse is insensitive to the pulse width for widths up to 1 time slot.

The curves for Gaussian-shaped input pulses imply very strong sensitivity of required energy per pulse to pulse width. This is a consequence of the rapid falloff of the spectrum of a Gaussian pulse with frequency. It is suspected that, although for certain fiber systems the received pulses may appear approximately Gaussian in the time domain, the frequency spectrum will not suffer such a rapid falloff. The results for the exponential-shaped input pulses seem much more realistic.

For exponential-shaped optical pulses we notice, from Figs. 15 and 16, that the shot noise coefficients I_1 and $\sum_1$ are sensitive to the optical

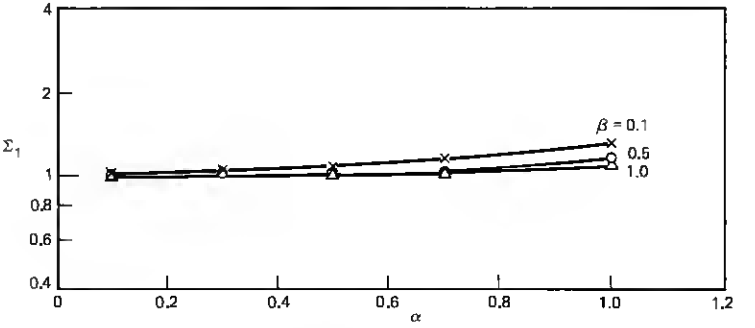

Fig. 8—Rectangular family Σ_1 vs α and β.

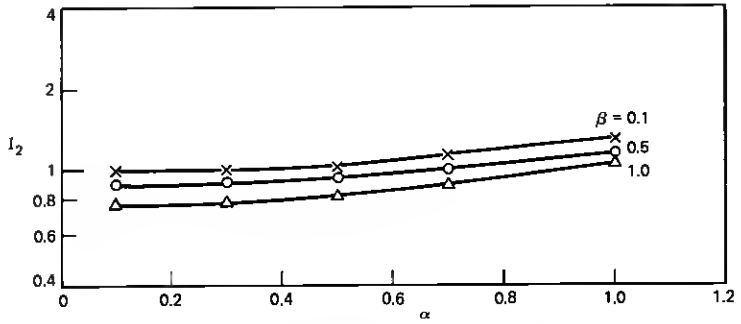

Fig. 9—Rectangular family I_2 vs α and β.

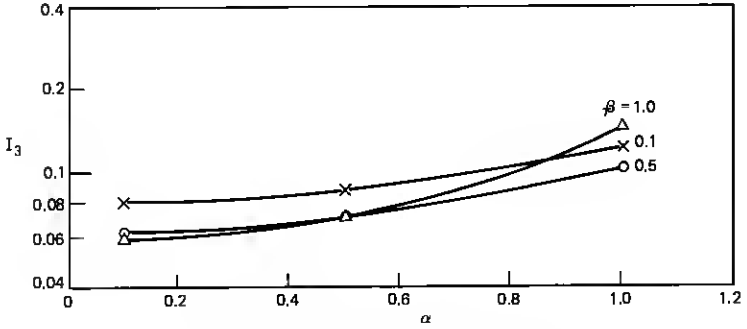

Fig. 10—Rectangular family I_3 vs α and β.

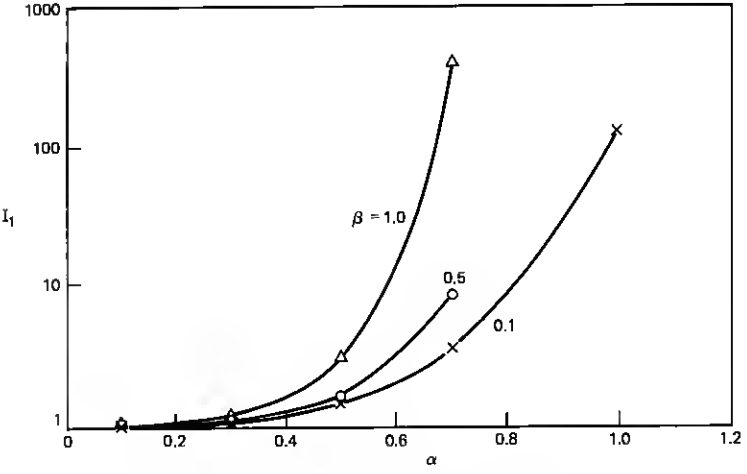

Fig. 11—Gaussian family I_1 vs α and β.

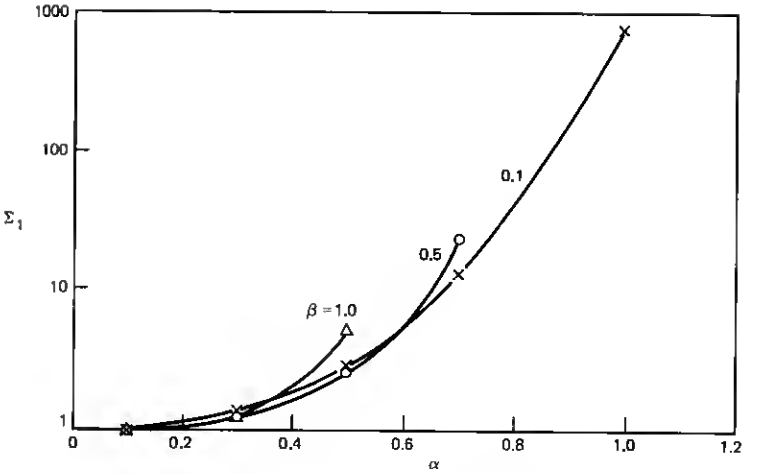

Fig. 12—Gaussian family Σ_1 vs α and β.

pulse width, but that these sensitivities imply a practically useful tradeoff in required optical power vs allowable bit rate. That is, one might take a certain power penalty to allow equalization which can substantially increase the usable bit rate on a channel having a fixed optical output pulse width. The sensitivity of I_2 and I_3 to the optical pulse width is similar to that of $\sum_1$ and less significant because in-

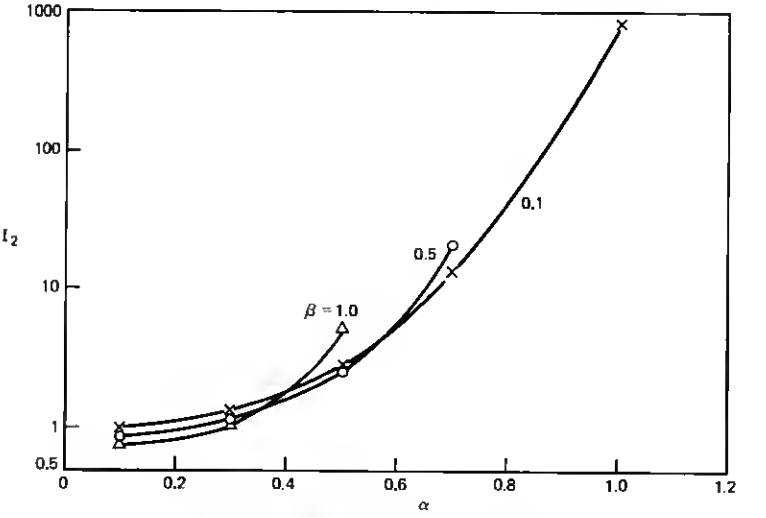

Fig. 13—Gaussian family I_2 vs α and β.

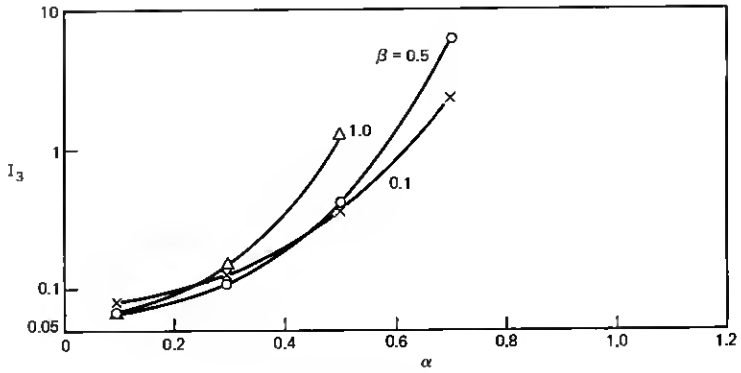

Fig. 14—Gaussian family I_3 vs α and β.

creases in the thermal noises of the receiver are for the most part compensated for by adjustment of the avalanche gain, with only a small penalty in excess shot noise. The above statements will be made quantitative in Section VI.

VI. OBTAINING THE RELATIONSHIPS FOR FIXED ERROR RATE BETWEEN THE REQUIRED ENERGY PER PULSE, OPTIMAL AVALANCHE GAIN, AND OTHER PARAMETERS

Suppose that in (23) all parameters are fixed except $\langle g \rangle$, $\langle g^2 \rangle$, $b_{\min}$, and $b_{\max}$.

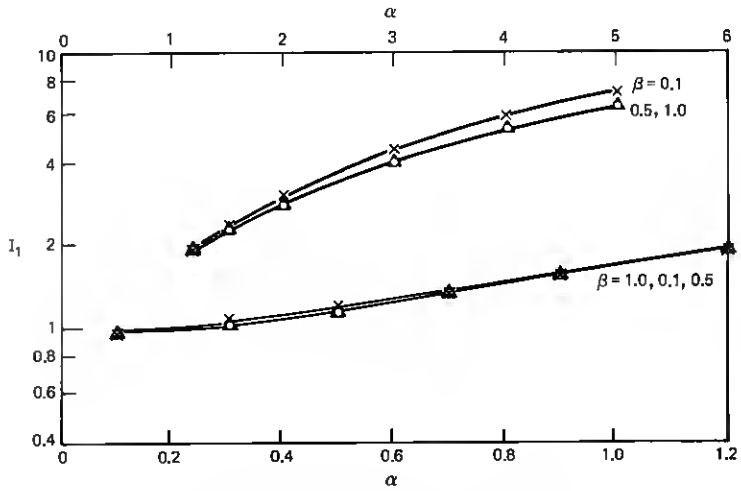

Fig. 15—Exponential family I_1 vs α and β.

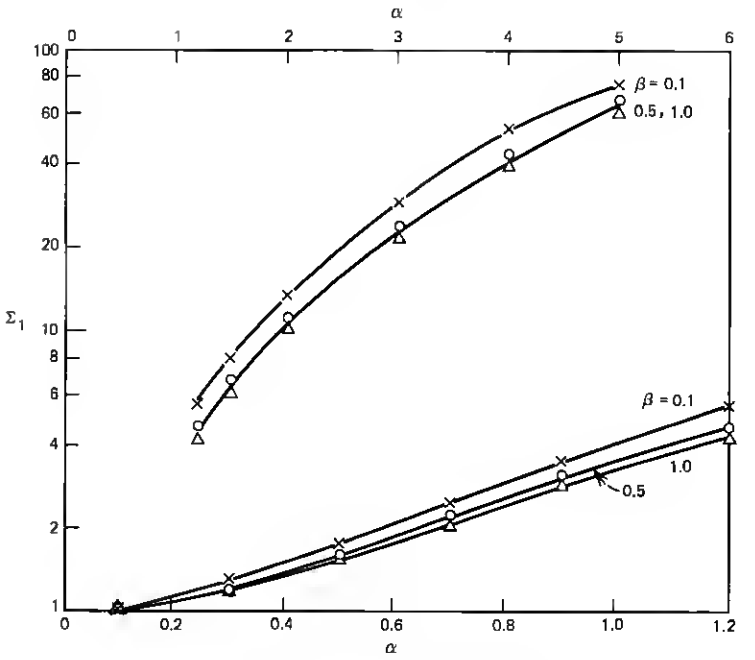

Fig. 16—Exponential family Σ_1 vs α and β.

The receiver equalized output at the sampling time, due to an optical pulse of energy b_0, is b_0.

When $b_0 = b_{\min}$, we must be sure that the prohability that noise drives the receiver output $v_{out}(t)$ at the sampling time ahove the threshold D is less than 10^{-9}.† Using the signal-to-noise ratio approximation,‡ we require the noise variance, $NW(b_{\min})$, to he less than $\{\frac{1}{6}[D - b_{\min}]\}^2$.

Therefore, we require that

$$NW(b_{\min}) \leqq \frac{1}{36}[D - b_{\min}]^2. \tag{26}$$

Furthermore, when $b_0 = b_{\max}$ we must he sure that the prohability that the noise drives the receiver output helow the threshold is less than 10^{-9}. Therefore, we require that

$$NW(b_{\max}) \leqq \frac{1}{36}[b_{\max} - D]^2. \tag{27}$$

† An error rate of 10^{-9} is arbitrarily chosen here. Dependence of required optical power on error rate is discussed in Part II of this paper.

‡ See Appendix A.

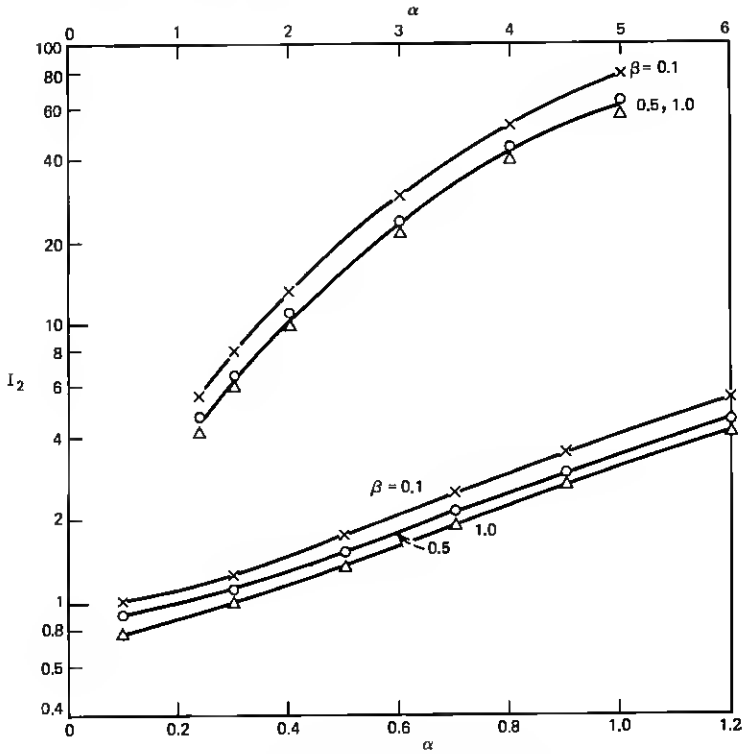

Fig. 17—Exponential family I_2 vs α and β.

Using equality in (26) and (27), we require for a 10^{-9} error rate

$$\sqrt{NW(b_{\max})} + \sqrt{NW(b_{\min})} = \tfrac{1}{6}(b_{\max} - b_{\min}). \tag{28}$$

Very often we have a fixed ratio $(b_{\min}/b_{\max}) = \rho$.

Rearranging (28) we obtain

$$b_{\max} = \frac{6}{1-\rho}\left[\sqrt{NW(b_{\max})} + \sqrt{NW(\rho b_{\max})}\right]. \tag{29}$$

In order to obtain numerical results, we shall make the following reasonable assumptions. Let the dark current be negligihle and let $b_{\min}/b_{\max}$ be much less than unity. Therefore we shall set $\lambda_0 = 0$, $b_{\min} = 0$.† We obtain from (23)

† Quantitative discussion of the consequences of these approximations are given in Part II.

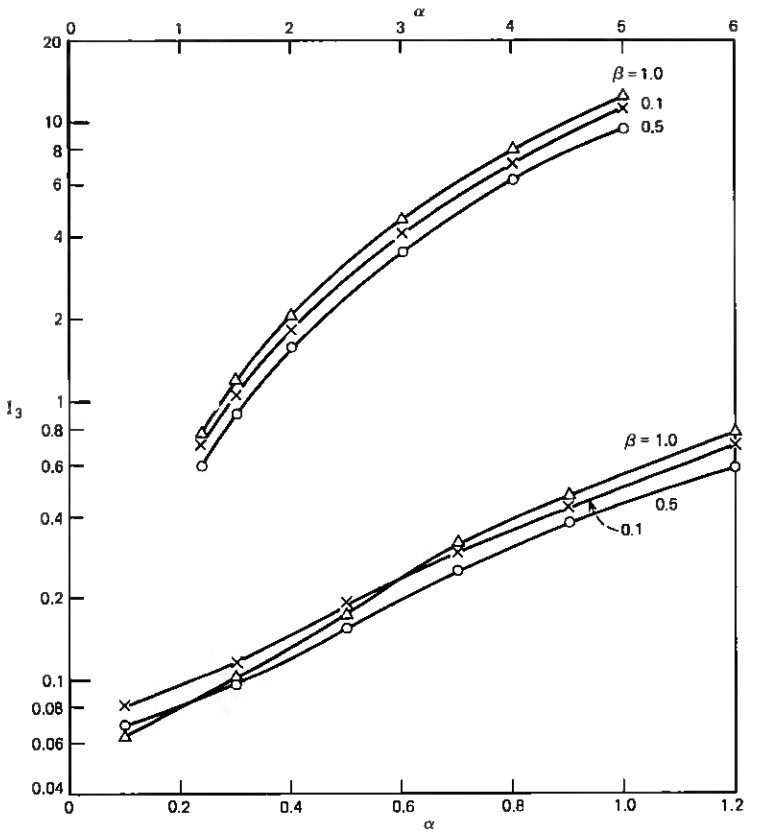

Fig. 18—Exponential family I_3 vs α and β.

$$NW(b_0) \cong \left[\frac{\hbar\Omega}{\eta}\right]^2 \left\{\frac{\langle g^2\rangle}{\langle g\rangle^2}\frac{\eta}{\hbar\Omega}\left[b_0 I_1 + b_{\max}(\Sigma_1 - I_1)\right] + \frac{1}{\langle g\rangle^2}[Z]\right\},$$

where

$$Z \triangleq \left\{\frac{T}{e^2}\left[S_I + \frac{2k\theta}{R_b} + \frac{S_E}{R_T^2}\right] I_2 + \frac{(2\pi C_T)^2}{Te^2} S_E I_3\right\}. \tag{30}$$

In (30), Z includes all the thermal noise terms of (23).

From (29), taking the limit as $\rho \to 0$ ($b_{\min} \to 0$), we obtain the conditions to achieve a 10^{-9} error rate as follows.

Case I: Thermal noise (Z) dominates (i.e., little or no avalanche gain).

$$b_{\max} = \frac{12\hbar\Omega}{\eta\langle g\rangle} Z^{\frac{1}{2}}. \tag{31}$$

Case II: Optimal gain (i.e., $\langle g \rangle$ adjusted to minimize the required optical energy in an "on" pulse b_{max}).

Let the relationship between $\langle g^2 \rangle$ and $\langle g \rangle$ he specified in the usual way:

$$\langle g^2 \rangle = \langle g \rangle^{2+x}, \tag{32}$$

where x depends upon the type of detector. We ohtain the following formula for the optimal gain:

$$\langle g \rangle_{optimal} = (6)^{-1/(1+x)}(Z)^{1/(2+2x)}(\gamma_1)^{1/(2+2x)}(\gamma_2)^{-1/(1+x)}, \tag{33}$$

where defining $I_5 = \sum_1 - I_1$ [see eq. (23)]

$$\gamma_1 \triangleq \frac{-[\sum_1 + I_5] + \sqrt{(\sum_1 + I_5)^2 + \frac{16(1+x)}{x^2}\sum_1 I_5}}{2\sum_1 I_5} \tag{34}$$

$$\gamma_2 \triangleq \sqrt{1/\gamma_1 + I_5} + \sqrt{1/\gamma_1 + \sum_1}.$$

We obtain the following formula for b_{max}:

$$b_{max} = \frac{\hbar\Omega}{\eta}(6)^{(2+x)/(1+x)}(Z)^{x/(2+2x)}(\gamma_1)^{x/(2+2x)}(\gamma_2)^{(2+x)/(1+x)}. \tag{35}$$

That is,

$$b_{max} \propto [Z]^{x/(2+2x)}. \tag{36}$$

We therefore see that for these assumptions and $x = 0.5$ corresponding to a silicon avalanche detector the minimum required energy per pulse varies as the one-half power of the thermal noise term, Z, without avalanche gain, and as the one-sixth power of the thermal noise term, Z, with optimal gain.

However, this does not mean that at optimal gain the value of Z is unimportant. By reducing Z (the thermal noise terms) through proper choice of hiasing and amplifier circuitry, we still minimize the optimizing avalanche gain [see (33)] and ohtain some reduction in the required energy per pulse (see Part II).

6.1 *Example*

From eqs. (23), (30), (34), and (35) we can calculate, for various shaped optical pulses, the effect of intersymbol interference on the required energy per "on" pulse (b_{max}) and therefore on the required average optical power needed for a 10^{-9} error rate.† We shall assume

† That is, if pulses are "on" half the time, the required optical power equals $b_{max}/2T$.

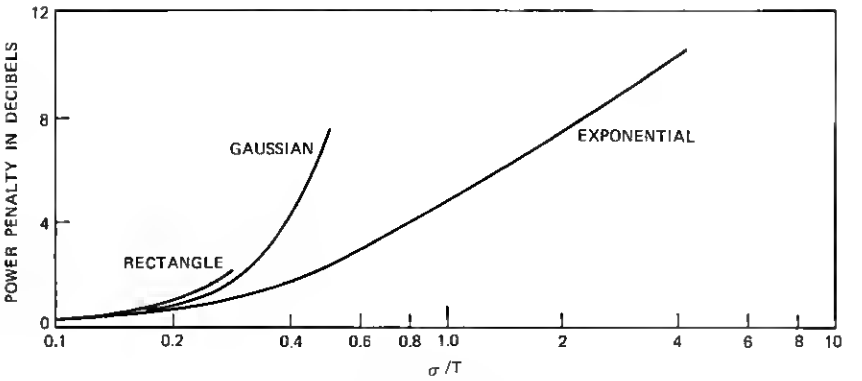

Fig. 19—No avalanche gain.

that the detector amplifier shunt resistance R_T is sufficiently large so that the term $((2\pi C_T)^2/Te^2)S_E I_3$ dominates the thermal noise in (23) and (30).

The minimal required optical power is obtained for very narrow optical input pulses.† For other pulse shapes, the *excess* required optical power can be defined as a *penalty* in dB for not using narrow pulses. This penalty is plotted in Figs. 19 and 20 for the case of no avalanche gain and optimal avalanche gain using the pulse shapes of (25), assuming a silicon detector ($x = 0.5$). In those figures, the abscissa is the normalized rms optical pulse width defined as follows:

$$\frac{\sigma^2}{T^2} = \frac{\left(\int t^2 h_p(t)dt\right) - \left(\int t h_p(t)dt\right)^2}{T^2}, \tag{37}$$

where T = time slot width.

VII. CONCLUSIONS

7.1 *Conclusion on Choosing the Biasing Circuitry*

From the results of Sections IV and VI, and from (23), it is clear that, to minimize the thermal noise degradations introduced by the amplifiers following the detector, it is necessary to make the amplifier input resistance and the biasing circuit resistance sufficiently large so that the amplifier series noise source dominates the Johnson noise of these parallel resistances. When designing the amplifier, one should keep in mind that for a silicon avalanche detector the required optical

† See Appendix B.

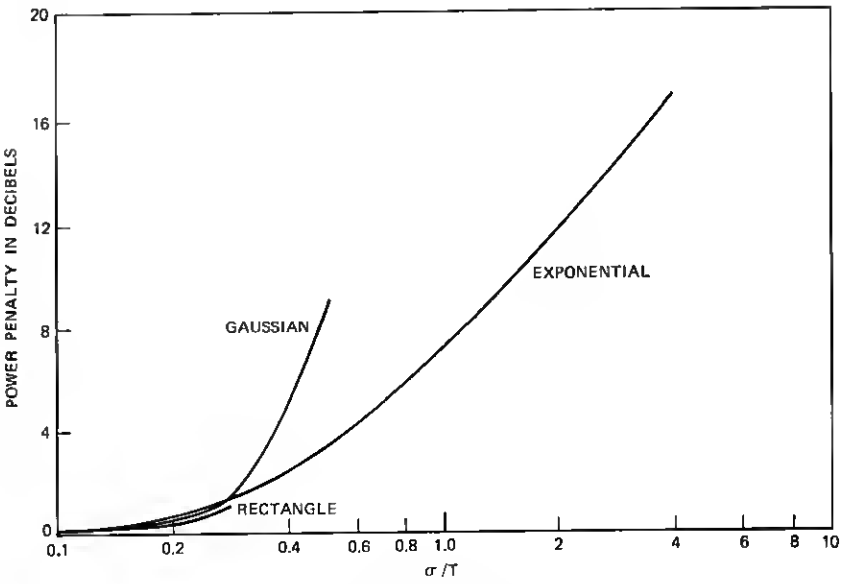

Fig. 20—Optimal gain.

energy per pulse at optimal gain varies roughly as the one-sixth power of the thermal noise variance at the receiver output, and therefore it is not wise to spend too much money on thermal noise reduction. On the other hand, if one is not using avalanche gain, the required energy per pulse varies roughly as the one-half power of the thermal noise variance at the receiver output.

In order to minimize the effects of the thermal noise, the total capacitance shunting the detector should be as small as possible and the equivalent series thermal noise source of the amplifier should also be as small as possible.

7.2 *The Effect of Bit Rate on Required Energy Per Pulse*[†]

The effect of bit rate on the required energy per pulse is small if the received pulses remain well confined to a time slot. In (23), assume I_1, $\sum_1$, I_2, and I_3 are fixed corresponding to a fixed received pulse width relative to a time slot. Then the shot noise terms due to the signal are independent of the bit rate $1/T$, and the shot noise due to the dark current decreases with increasing bit rate. If the series noise from the amplifier dominates, then the thermal noise increases with increasing

[†] This subject will be discussed in more detail in Part II.

bit rate, but is for tbe most part compensated for by the avalanche gain witb little penalty in required energy per pulse.

If considerable equalization is being used, tben tbe required energy per pulse increases with the hit rate (hecause a higher bit rate necessitates greater equalization). For the equalization assumed above, where the equalized pulses are forced to go to zero at all sampling times except one, tbe required energy per pulse is a strong function of the hit rate. For example, with exponential-shaped received pulses, the required optical power at optimal avalanche gain was roughly 6 dB higher for a pulse 1 time slot wide to the $1/e$ point compared to a pulse only 0.25 time slot wide to the $1/e$ point (see Fig. 20).

On the otber hand, it is clear that zero-forcing-type equalization is not optimal, particularly for received pulses whose spectra fall off rapidly with frequency. It is more likely that some compromise hetween eye opening and output noise variance results in minimum required energy per pulse.

For tbe assumed zero-forcing equalization, we still can conclude that a usable tradeoff exists between required energy per pulse and bit rate, and this will allow some extension of the usable rate on "dispersion-limited" fibers.

7.3 *Comments on Previous Work*

The purpose of this paper has heen to illustrate the application of the "high-impedance" front-end design to optical digital repeaters, to take into account precisely the input pulse shape and the equalizer-filter shape, and to obtain explicit formulas for the required optical power to achieve a desired error rate as a function of the other parameters.

Previous autbors[12,13] working in tbe areas of particle counting and video amplifier design have recognized that a higb-impedance front end followed by proper equalization in later stages provides low noise and adequate bandwidth. However, optical communication theorists[5,6,14,15] have in the past often used the criterion "$RC \leqq T$"–loading down the front-end amplifier so as to have adequate handwidth without equalization–therein incurring an unnecessary noise penalty. Some optical experimenters[16,17] have recognized the bigb-impedance design for observing isolated pulses or single frequencies, but failed to recognize the use of equalization.

Many previous authors[3,4,6,15] have used simple formulas (whicb usually assume isolated rectangular input pulses and a front-end handwidth of the reciprocal pulse width) to obtain the required power in

optical communication systems for a desired signal-to-noise ratio. Often these formulas average out the signal-dependent nature of the shot noise. If modified to include the high-impedance design concept, such formulas are very useful for obtaining "hall park" estimates of optical power requirements. Such formulas are, in general, special cases of the formulas described here.

7.4 *Experimental Verification*

In work recently reported,[18] J. E. Goell bas shown that, in a 6.3-Mb/s repeater operating at an error rate of 10^{-9}, agreement of experimentally determined power requirements and the ahove theory were within 1 dB (0.25 dB in cases without avalanche gain). In particular, using an FET front end and the "high-impedance" design, the optical power requirement without avalanche gain was 8 dB less than with the front end loaded down to tbe "$RC = T$" design.

APPENDIX A

Signal-to-Noise Ratio Approximation

In this paper we bave calculated the mean voltage ($b_{\max}$ or $b_{\min}$) and the average-squared deviation from the mean voltage ($NW(b_{\max})$ or $NW(b_{\min})$) at the receiver output at the sampling times. In order to calculate error rates, we shall assume that the output voltage is approximately a Gaussian random variahle. This is the signal-to-noise ratio approximation. Thus if the threshold, to which we compare the output voltage, is D, and if the desired error prohability is P_e, we have

$$\frac{1}{\sqrt{2\pi\sigma_o^2}} \int_D^\infty \exp\left[-(v - b_{\min})^2/2\sigma_o^2\right] dv = P_e, \tag{38}$$

where

$$\sigma_o^2 = NW(b_{\min})$$

and

$$\frac{1}{\sqrt{2\pi\sigma_1^2}} \int_{-\infty}^D \exp\left[-(v - b_{\max})^2/2\sigma_1^2\right] dv = P_e,$$

where

$$\sigma_1^2 = NW(b_{\max}).$$

Changing the variables of integration we obtain tbe following expressions, equivalent to (38):

$$\frac{1}{\sqrt{2\pi}} \int_Q^\infty e^{-x^2/2} dx = P_e, \tag{39}$$

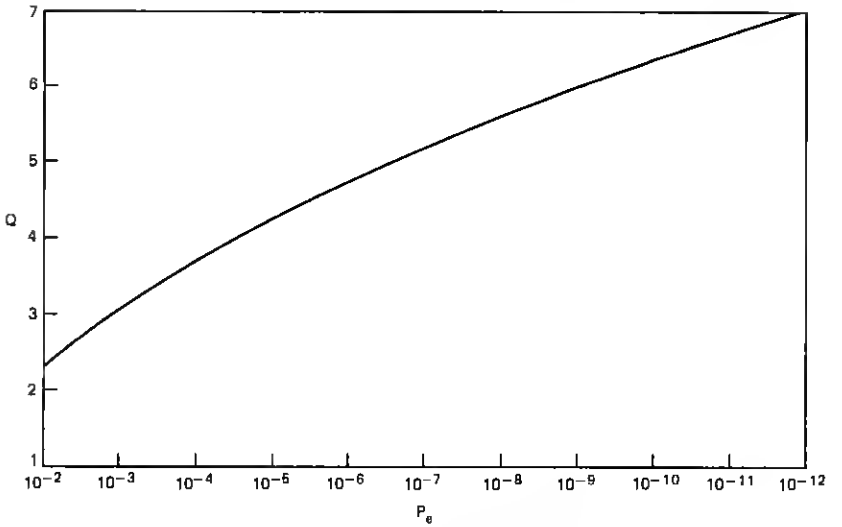

Fig. 21—Q vs P_e, $P_e = \frac{1}{\sqrt{2\pi}} \int_Q^\infty e^{-x^2/2} dx$.

where

$$Q = (D - b_{\min})/\sigma_o$$

and also

$$Q = (b_{\max} - D)/\sigma_1.$$

Thus we must have

$$\sigma_o = \sqrt{NW(b_{\min})} = (D - b_{\min})/Q$$

and

$$\sigma_1 = \sqrt{NW(b_{\max})} = (b_{\max} - D)/Q.$$

Therefore we must also have (eliminating D)

$$\sqrt{NW(b_{\max})} + \sqrt{NW(b_{\min})} = (b_{\max} - b_{\min})/Q.$$

The value of Q is determined by the error rate through (39) above. Figure 21 shows a plot of Q vs P_e which can be obtained from standard tables.

Equation (39) states that the threshold must be Q standard deviations (of the noise at $b_{\min}$) above $b_{\min}$, and also must be Q standard deviations (of the noise at $b_{\max}$) below $b_{\max}$ to insure the desired error rate. For an error rate of 10^{-9} ($P_e = 10^{-9}$) Q is roughly 6 (5.99781).

APPENDIX B

Optimal Input Pulse Shape

We now wish to show that the optimal input pulse, $h_p(t)$ shape (which minimizes the required average optical power) is ideally an impulse; and for practical purposes a pulse which is sufficiently narrow so that its Fourier transform is almost constant for all frequencies passed by the receiver. To do this, we shall show that such a narrow pulse minimizes the noises $NW(b_{\max})$ and $NW(b_{\min})$ defined in (23).

We begin with the already established condition that the area of $h_p(t)$ is equal to unity and that $h_p(t)$ is positive (power must, of course, be positive).

$$\int h_p(t)dt = 1; \qquad h_p(t) > 0. \tag{40}$$

These conditions imply the following weaker condition:

$$|H_p'(f)| = \left| \int h_p(t)e^{-i2\pi ft/T}dt \right|$$

$$\leqq \int |h_p(t)|\,|e^{-i2\pi ft/T}|dt = \int h_p(t)dt = H_p'(0) = 1. \tag{41}$$

Consider first the thermal noise terms of (23) involving the integrals I_2 and I_3:

$$I_2 = \int \frac{|H_{\text{out}}'(f)|^2}{|H_p'(f)|^2}\,df; \qquad I_3 = \int \frac{|H_{\text{out}}'(f)|^2}{|H_p'(f)|^2}\,f^2df. \tag{42}$$

Using (41) in (42) we see that these terms I_2 and I_3 are minimized for any desired output pulse $H_{\text{out}}'(f)$ by setting $|H_p'(f)| = H_p'(0) = 1$ for all frequencies, f, for which $|H_{\text{out}}'(f)| > 0$. Thus, ideally, to minimize I_2 and I_3, $h_p(t)$ is an impulse of unit area which also satisfies the conditions (40).

We must now show that the shot noise terms of (23), I_1 and $\sum_1 - I_1$, are minimized by a very narrow pulse $h_p(t)$.

First recall that $(\sum_1 - I_1)b_{\max}(\hbar\Omega/\eta)\langle g^2\rangle/\langle g\rangle^2$ is the worst-case, mean-square shot noise at the sampling time due to all other pulses except the one under decision, and assuming all of those pulses are "on" ($b_k = b_{\max}$ for $k \neq 0$). Thus, from (17), we obtain

$$\sum_1 - I_1 \geqq 0, \tag{43}$$

where

$$\sum_1 - I_1 = \int \Big(\sum_{k\neq 0} h_p(t' - kT)\Big)h_I^2(-t')dt'$$

and where $h_I(t)$ is the overall receiver impulse response relating $h_p(t)$ to $h_{out}(t)$.

Now let the optical pulse $h_p(t)$ be an impulse of unit area. Then the overall impulse response h_I must be equal to $h_{out}(t)$ and therefore using (43) and (9) we obtain

$$\sum_1 - I_1 = \sum_{k \neq 0} h_{out}^2(-kT) = 0 \quad (\text{for } h_p(t) = \delta(t)). \tag{44}$$

Because condition (9) requires zero-crossing equalization, we have shown that an impulse shape for $h_p(t)$ minimizes (removes) the shot noise from pulses other than the one under decision.

Finally, consider the shot noise from the pulse under decision given by $I_1(\hbar\Omega/\eta)b_o\langle g^2\rangle/\langle g\rangle^2$ where

$$I_1 = \int h_p(t')h_I^2(-t')dt' > 0. \tag{45}$$

We already have the condition (9)

$$h_{out}(0) = \int h_p(t')h_I(-t')dt' = 1. \tag{46}$$

We can next use the Shwarz inequality on (46)

$$(h_{out}(0))^2 = 1 = \left(\int h_p^{\frac{1}{2}}(t)h_p^{\frac{1}{2}}(t)h_I(-t)dt\right)^2 \leqq \int h_p(t)dt \int h_p(t)h_I^2(-t)dt. \tag{47}$$

Since $\int h_p(t)dt = 1$, we have from (47) and (45)

$$I_1 \geqq 1. \tag{48}$$

Now set $h_p(t)$ equal to a unit area impulse. It then must follow from (46) that $h_I(0) = 1$. We finally obtain

$$\int h_p(t)h_I^2(t)dt = h_I^2(0) = 1. \tag{49}$$

From (48) and (49) we see that an impulse-shaped $h_p(t)$ makes I_1 achieve its minimum value of unity.

Summarizing, an impulse-shaped optical input pulse $h_p(t)$ (for practical purposes a sufficiently narrow pulse so that its Fourier transform is approximately constant for all frequencies passed hy the receiver) minimizes all the pulse-shape-dependent coefficients (I_1, $\sum_1 - I_1$, I_2,

and I_3) in the noise expression (23) and thereby minimizes the required average optical power to achieve a desired error rate (using the signal-to-noise ratio approximation of Appendix A).

REFERENCES

1. Personick, S. D., "Baseband Linearity and Equalization in Fiber Optic Communication Systems," to appear in B.S.T.J., September 1973.
2. Personick, S. D., "Statistics of a General Class of Avalanche Detectors with Applications to Optical Communication," B.S.T.J., *50*, No. 10 (December 1971), pp. 3075–3096.
3. Melchior, H., et al., "Photodetectors for Optical Communication Systems," Proc. IEEE, *58*, No. 10 (October 1970), pp. 1466–1486.
4. Pratt, W. R., *Laser Communication Systems*, New York: John Wiley and Sons, 1969.
5. Huhhard, W. M., "Comparative Performance of Twin-Channel and Single-Channel Optical Frequency Receivers," IEEE Trans. Commun. *COM20*, No. 6 (December 1972), pp. 1079–1086.
6. Anderson, L. K., and McCurtry, B. J., "High Speed Photodetectors," Proc. IEEE, *54* (Octoher 1966), pp. 1335–1349.
7. McIntyre, R. J., "Multiplication Noise in Uniform Avalanche Diodes," IEEE Trans. Electron Devices, *ED-13*, No. 1 (January 1966), pp. 164–168.
8. Melchior, H., and Lynch, W. T., "Signal and Noise Response of High Speed Germanium Photodiodes," IEEE Trans. Electron Devices, *ED-13* (Decemher 1966), pp. 829–838.
9. Klauder, J. R., and Sudarshan, E. C. G., *Fundamentals of Quantum Optics*, New York: W. A. Benjamin, Inc., 1968, pp. 169–178.
10. Parzen, E., *Stochastic Processes*, San Francisco: Holden-Day, 1962, p. 156.
11. Figure 5h is from *Transmission Systems for Communication*, Bell Telephone Lahoratories, 1970, p. 651.
12. Gillespie, A. B., *Signal, Noise, and Resolution in Nuclear Particle Counters*, New York: Pergamon Press, Inc., 1953.
13. Schade, O. H., Sr., "A Solid-State Low-Noise Preamplifier and Picture-Tube Drive Amplifier for a 60 MHz Video System," RCA Rev., *29*, No. 1 (March 1968), p. 3.
14. Chown, M., and Kao, K. C., "Some Broadhand Fiber-System Design Considerations," ICC 1972 Conf. Proc., June 19–21, 1972, Philadelphia, Pa., pp. 12–1, 12–5.
15. Ross, M., *Laser Receivers*, New York: John Wiley and Sons, 1967, p. 328.
16. Edwards, B. N., "Optimization of Preamplifiers for Detection of Short Light Pulses with Photodiodes," Appl. Opt. *5*, No. 9 (September 1966), pp. 1423–1425.
17. Mathur, D. P., McIntyre, R. J., and Wehh, P. P., "A New Germanium Photodiode with Extended Long Wavelength Response," Appl. Opt., *9*, No. 8 (August 1970), pp. 1842–1847.
18. Goell, J. E., work to be presented at the Conference on Laser Engineering and Applications (CLEA) Washington, D.C., May 30–June 2, 1973.